Dendrochronologia 84 (2024) 126177

Contents lists available at ScienceDirect

Dendrochronologia

journal homepage: www.elsevier.com/locate/dendro

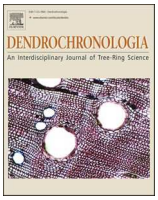

Blue intensity measurements in a South American conifer: evaluation of different methodological approaches for *Araucaria araucana*

Ignacio A. Mundo [a,b,*], Ricardo Villalba [a], Silvina Velez [a], Rob Wilson [c]

[a] Laboratorio de Dendrocronología e Historia Ambiental, IANIGLA-CONICET, Mendoza, Argentina
[b] Facultad de Ciencias Exactas y Naturales, Universidad Nacional de Cuyo, Mendoza, Argentina
[c] School of Earth & Environmental Sciences, University of St. Andrews, St. Andrews, UK

ARTICLE INFO

Keywords:
(up to 6): blue intensity
Araucaria araucana
Patagonia
Wood density
Tree rings

ABSTRACT

Blue intensity (BI) has emerged as an inexpensive and relatively simple method for obtaining a proxy for relative wood density, and it has been successfully tested on several conifer species in Europe, North America, Asia and Australasia. Despite international efforts to promote the use of these methods worldwide, BI chronologies developed for native South American species have not yet been published. The possibility of developing BI chronologies in *Araucaria araucana*, an emblematic conifer of northern Patagonia, began to be explored some years ago. However, as it has been reported in other species, the wood anatomy of *Araucaria* presents several difficulties for obtaining robust BI common signals between samples. Therefore, we conducted this study to assess various methods for determining BI parameters based on the degree of common signal between trees in the chronology and their correlation with climatic factors. In this study, we demonstrated the feasibility of developing reliable BI chronologies from a site within the *Araucaria* range in Argentina by analysing the sensitivity to changes in the width of the measurement window. Although replicating measurements within the same core improved the classical statistic used to quantify the expressed population signal in a chronology (i.e. EPS), the results obtained here show that the chronologies developed using different methods were practically identical. Furthermore, our results revealed different climate signals expressed by both earlywood (EWBI) and latewood (LWBI) BI records, corresponding to the current spring and summer, respectively. In addition, soil water availability was significantly associated with wood density variation. Therefore, the climatic and environmental information provided by BI measurements in *Araucaria* complements what is already known from ring width (RW) and thus highlights its potential for use in future climate and ecological reconstructions.

1. Introduction

Blue intensity (BI) is generally an inexpensive and simple method to obtain a proxy for relative wood density (Björklund et al., 2014; McCarroll et al., 2002). Based on these advantages over traditional x-ray-based measurements, the utilisation of BI and the number of papers applying this method has exponentially increased over the last couple of decades demonstrating the wide possibilities of this methodology for accurately capturing density variations in tree rings (Kaczka and Wilson, 2021). BI parameters have been used, analogous to the maximum wood density (MXD) in tree rings, almost exclusively as indicators of summer temperature from high elevation/latitude sites in the Northern Hemisphere. Geographically, BI parameters, tested on >20 conifer species across Europe, North America, Asia and Australasia, have demonstrated the broad potential of this method for capturing wood density (Kaczka and Wilson, 2021; Björklund et al., *in submission*). Despite international efforts to promote the use of BI worldwide through the recent establishment of the International Blue Intensity Network Development (I-BIND) Working Group, under the auspices of the Association of Tree-Ring Research, no BI chronologies have yet been published for native South American species.

Araucaria araucana is an emblematic conifer in northern Patagonia. It is a very long-lived species: individuals have been dated to be over 1000 years old (Aguilera-Betti et al., 2017). Edmund Schulman from the Laboratory of Tree-Ring Research (LTRR) of the University of Arizona, a pioneer in the dendrochronological study of this species, conducted a

* Corresponding author at: Laboratorio de Dendrocronología e Historia Ambiental, IANIGLA-CONICET, Mendoza, Argentina.
E-mail addresses: iamundo@mendoza-conicet.gob.ar (I.A. Mundo), ricardo@mendoza-conicet.gob.ar (R. Villalba), silvinave@gmail.com (S. Velez), rjsw@st-andrews.ac.uk (R. Wilson).

https://doi.org/10.1016/j.dendro.2024.126177
Received 3 December 2023; Received in revised form 30 January 2024; Accepted 5 February 2024
Available online 8 February 2024

reconnaissance trip in Argentina and Chile between 1949 and 1950. He highlighted the potential of *Araucaria* for dendroclimatological studies based on the environmental conditions in which the species grows: sites with marked climatic seasonality and water limitation (mainly rocky hillocks in foothills-plains with pure stands in the eastern limit of distribution). Based on his extensive experience in the Rocky Mountains, he suggested that the environmental conditions in which *Araucaria* grew were a good indication of sites dry enough to provide promising drought-sensitive chronologies (Schulman, 1956). Since the 1970s, with the second expedition of the LTRR (LaMarche et al., 1979) to South America, a large number of ring width (RW) *Araucaria* chronologies have been developed that have facilitated the analyses of the climate-radial growth relationship of the species (Hadad et al., 2015; Mundo et al., 2012b; Veblen et al., 1995), the development of hydroclimatic (drought indices: Morales et al., 2020, streamflow: Holmes et al., 1979; Mundo et al., 2012a), temperature (Neukom et al., 2014; Villalba et al., 1989), atmospheric circulation (Villalba et al., 2012) and ecological reconstructions (age structure: Hadad et al., 2020; Mundo, 2011; fire history: González et al., 2005; Mundo et al., 2013; impact of reproductive efforts on radial growth and reconstruction of masting events: Hadad et al., 2021; Mundo et al., 2021; Rozas et al., 2019). However, all these climatic reconstructions or ecological inferences were based on RW and, to date, no wood density chronologies have been published. This situation is also shared with other Patagonian conifers (*Austrocedrus chilensis*, *Fitzroya cupressoides*) for which climatic relationships have been identified on the basis of RW (Lara and Villalba, 1993; Villalba, 1990; Villalba et al., 1998; Villalba and Veblen, 1997) or stable isotopes (Lavergne et al., 2018). This situation is related to the lack of densitometric capabilities in the dendrochronological laboratories of Argentina and Chile.

The possibility of developing BI chronologies in *Araucaria* began to be explored seven years ago (Mundo et al., 2016). As a first step, X-ray density and BI series were compared, finding a high degree of common synchrony at the individual level (Fig. S1), although not as high as noted for some northern hemisphere species (Kaczka et al., 2018; Wilson et al., 2014). However, the wood anatomy of this species showed difficulties, such as rings with curved or wavy edges and wide rays, making it challenging to obtain robust BI common signals between samples (Fig. S2). Despite the relatively homogeneous wood colouring with no contrast between sapwood and heartwood (Diaz-Vaz et al., 2002; Tortorelli, 1956), the presence of fungal staining is the main limitation for extracting robust BI data without any long-term trend biases (Fig. 1). Can the size and position of the BI windows be used to solve this problem and improve the robustness of the common BI signal in *Araucaria*? The lack of experience and protocols for dealing with these BI limitations in other species justified the need to develop a methodological pilot study to define measurement protocols. Consequently, the objectives of this study were: 1) to evaluate different approaches for obtaining BI parameters in *Araucaria* in relation to the degree of common signal of the chronologies and 2) to comparatively analyse their relationship with climatic parameters.

2. Materials and methods

2.1. Sample selection, processing and methodological approach

For this methodological pilot study, 60 *Araucaria* cores (30 trees) from the Ea. Nahuel Mapi site in Neuquén province (39°32'46.8 "S, 71°02'37.0 "W), which were used for the development of a ring-width chronology in Mundo et al. (2012b), were pre-selected for BI measurement. This forest stand, located at 1531 m a.s.l. on a rocky and stable substrate on the slopes of the Patagonian Andes, was sampled in December 2007. On this site, the mean annual precipitation is 639 mm and the mean annual temperature is 6.8 °C (Worldclim Global Climate Data). All the sampled cores were mounted on wooden mounts, sanded to 1000 grit, and archived in the Laboratorio de Dendrocronología e

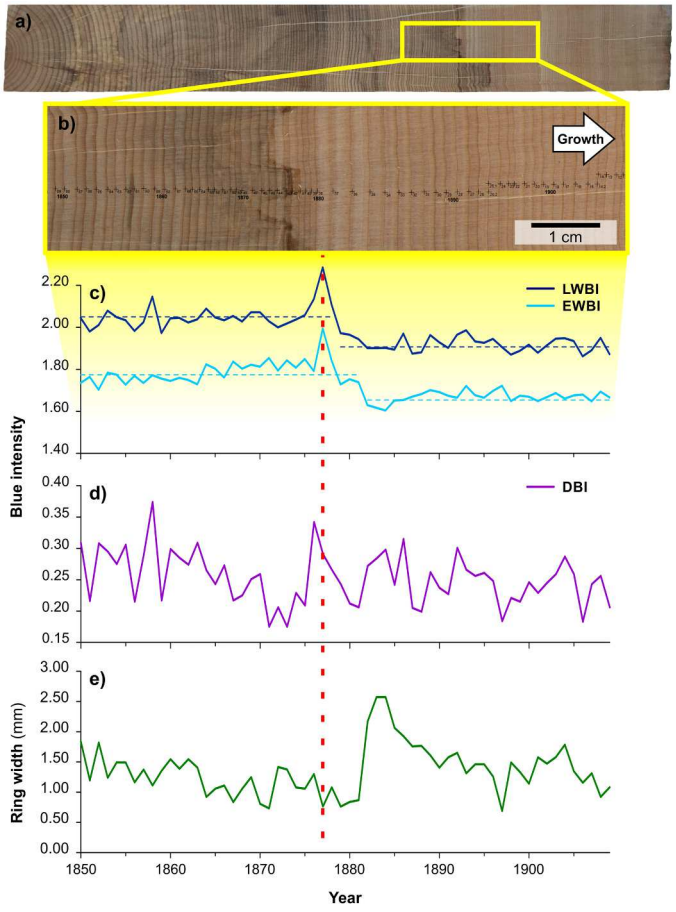

Fig. 1. Effect of fungal staining on the BI signal in *Araucaria*. a) and b) sample of *Araucaria* wood showing fungal staining from the pith (on the left) up to the year 1877. b) Enlargement for the period 1850–1910 showing the BI and RW measurement coordinate points using CooRecorder. The earlywood (EWBI) and latewood (LWBI) BI time series in c) show the change in the means (horizontal dashed-line) before and after 1877 (indicated by a red vertical dashed-line). This effect is minimised in the delta BI (DBI, d) values. Ring widths (RW, e) show a release few years after the colour change. The release is not related to fungal staining.

Historia Ambiental of IANIGLA-CONICET (LDHA, Mendoza, Argentina) collection. For the BI measurements, the samples were selected if they met the following criteria: no noticeable staining or colour changes, relatively well-defined rings and with a starting date of at least 1800. These criteria reduced the number of samples to 20 cores from 14 different trees.

Since the xylem of *Araucaria* xylem does not contain resin ducts, no pretreatment with acetone or ethanol was performed. Consequently, all selected samples were scanned on an Epson V550 flatbed scanner with 2400 dpi resolution. An IT8 7/2 reflective card (X-Rite IT8.7/2–1993, MONR2017:06–01, version 2) was used in the i1-Profiler software (X-Rite, v1.7.1.2596) to generate a calibration profile (icc file). This profile was selected from the Epson scan software and was used during the scanning session for all samples. To avoid ambient light bias, a non-reflective black neoprene cloth was placed over the samples to cover the entire glazed surface during scanning (Rydval et al., 2014).

Ring width (RW) and BI were measured from scanned images with CooRecorder software (Larsson, 2020; v. 9.6). CooRecorder allows the extraction of several tree ring metrics (e.g., RW, BI) by placing coordinates based on the location of tree-ring boundaries on high-resolution images of transverse section of wooden samples (Heeter et al., 2022). In this software, BI values are often extracted from a frame of defined dimensions, relative to the ring boundary. For species with

wavy ring boundaries or the presence of fungal staining, such as *Araucaria*, the decision regarding the location of the point coordinates can be crucial for obtaining non-anomalous BI series. In this study, to generate the RW series, the coordinates were placed at the boundaries of the rings and aligned based of the trajectory of radii. Due to the undulating nature of the ring boundaries in *Araucaria*, the data-picking mode of CooRecorder was used with the 'H' cursor to accurately position the frames. Special attention was given to ensuring that the long sides of the 'H' were as parallel as possible to the ring boundary, enabling the data frame to be located within the ring without overlapping with the previous or subsequent rings (see Fig. S2 in the Supplementary Material for a better understanding of the methodology through an example). Consequently, two "pos" files were generated per series: one for the RW (called *RW.pos) and one for the BI series (*BI.pos).

Additionally, CooRecorder requires the definition of where and how the BI data will be generated. This involves specifying which part of the ring is measured (latewood, earlywood or full ring), the method for processing the data image (mean of sorted pixels vs mean of slices) and the specifications for frame geometry (location, size and shape). Among these specifications, the latter are the most sensitive for obtaining BI values. In this study, based on previous experience showing a low common signal strength in *Araucaria* BI series (Mundo et al., 2016), we decided to modify the window frame width (100 and 200) and the location of the coordinate points (data frame in a central position or duplicated in marginal positions of the core: left and right). This led to the evaluation of four methodological experiments for collecting BI (for both earlywood and latewood) within a ring (Fig. 2):

1. a central 100-pixel width data frame (C_{100}),
2. a central 200-pixel width data frames (C_{200}),
3. two 100-pixel width data frame located towards the left and right margins, ensuring there was no overlap between them (LR), and
4. the mean of the two LR BI values (Mean).

In the LR experiment, two sets of BI data were extracted for the location of the left (L) and right (R) BI-data frames, which were positioned on the left and right edges of the core image, respectively. These data were treated as two independent radii. Given the scan resolution (2400 dpi) and the core diameter (5 mm), 100 dpi and 200 dpi frame width correspond to approximately 21% and 42% of the core image width. In all methods, all other values related to the frame characteristics were kept constant (see Table S1 in the Supplementary Material for the specified values).

In this study, we refer to BI as the inverted values of blue light reflectance (BR), following the convention proposed by Björklund et al. (*in submission*). To achieve this, the BR series was inverted by multiplying each value by − 1 and then adding the constant 2.56 (related to the light intensity scale 0–255) to eliminate any negative values (Rydval et al., 2014). From the EWBI and LWBI series, and drawing on previous experience with other species (Björklund et al., 2014; Wilson et al., 2017), delta BI (DBI = LWBI - EWBI) was calculated.

Individual BI and RW data series were then converted to Tucson decadal format using CDendro. By examining the graph of all series and comparison with the images, we verified whether the anomalous jumps at the beginning of the series (close to the pith) corresponded to colour anomalies associated with fungal stains. If this was confirmed, the corresponding anomalous parts were removed from all BI (EWBI, LWBI and DBI) and RW series to ensure they all had the same temporal extent.

2.2. Chronology development and statistical analyses

Cross-dating of all time-series (using both RW and BI) was verified using COFECHA (Holmes, 1983) and CDendro. Detrending the age-related growth trend was undertaken using the programme ARSTAN (Cook and Holmes, 1986). As stated by Rydval et al. (2014) for many species, an initial increase in BI series, apparent in the juvenile period, is followed by a steady decrease thereafter. For this reason, an age-dependent smoothing spline (Melvin et al., 2007) was considered more appropriate due to its additional flexibility to adjust for early period trends. In this implementation, an initial cubic smoothing spline was fit to tree-ring measurement with a stiffness of 20 years. For each successive measurement, the stiffness is incremented by that ring index. This results in a spline that is 20-year flexible at the start of the series and grows progressively stiffer. This approach helps capture the initial rapid growth of a young tree with a flexible spline, which then progresses to a more rigid spline that can better model the steady growth commonly found in mature trees. Therefore, all RW and BI data herein were detrended using this approach. Detrended series were calculated as ratios, and chronologies developed using a bi-weight robust mean (Fritts, 1976; Schweingruber, 1988). Residual chronologies were produced in the same manner as the standard chronologies, but in this case the chronologies were residuals from autoregressive modelling of the standardized index series.

The quality of the chronologies was assessed by the mean correlation between all series (RBAR) and the expressed population signal (EPS). RBAR is a measure of the common variance between the single series in a chronology (Wigley et al., 1984). Running RBAR values illustrate changes in the strength of common signal in tree growth variations over

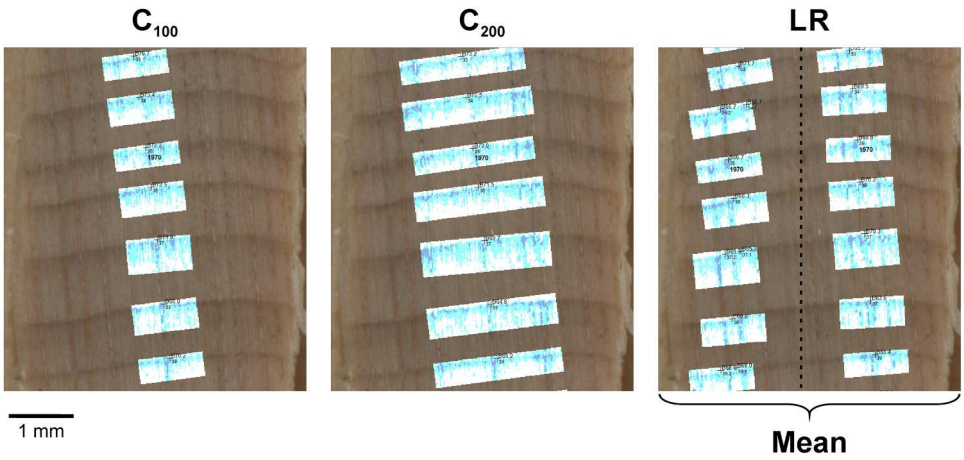

Fig. 2. Methodological approaches used in this study aimed to evaluate the effect of the size and location of the data frame for collecting BI. The different panels exemplify the four approaches applied to the same image to obtain BI values for latewood (C_{100}: a central 100-pixel width data frame; C_{200}: a central 200-pixel width data frame; LR: two 100-pixel width data frame located towards the left and right margins verifying the absence of overlapping of them; Mean: the mean of the LR BI values).

time. EPS measures how well the finite-sample chronology compares with a theoretical population chronology based on an infinite number of trees (Wigley et al., 1984). RBAR and EPS values were computed using a 20-year moving window with a 10-year overlap. The cutoff point for accepting EPS, as suggested by Wigley et al. (1984), is 0.85. The similarity between the BI residual chronologies from each treatment was analysed using correlation matrices. Correlation coefficients were also calculated between the different variants of residual chronologies obtained in the four methodological treatments for the three BI parameters and the RW residual chronology. Mean values per BI parameter were then calculated, and a summary correlation matrix was constructed.

2.3. Climatic influence on tree-ring parameters

Correlation functions (Blasing et al., 1984) were employed to determine the influence of climatic factors on the different tree-ring parameters. Drawing from previous experience with this species (Mundo et al., 2012b), correlation functions were computed between the residual tree-ring chronologies and different climatic variables (temperature, precipitation, Palmer Drought Severity Index) and atmospheric circulation indexes (sea surface temperature from El Niño 3 region, Antarctic Oscillation or Southern Annular Mode index). These correlations were computed for five quarter periods, starting with summer (December-February) of the previous growing season and ending with summer at the current growth year. Following Ols et al. (2023), the climatic data were detrended prior to climate-growth analyses using the same standardization curve (in this case, an age-dependent spline) as for the tree-ring series. The temperature record is from Bariloche (Servicio Meteorológico Nacional of Argentina; 41°09'S-71°15'W; period: 1931–2016), while the precipitation record is from Los Laureles (Dirección General de Aguas of Chile; 38°57'S, 72°12'W; period: 1947–2016). The Palmer Drought Severity Index (PDSI; Palmer, 1965) is a standardized measure of surface moisture conditions, ranging from about − 10 (dry) to + 10 (wet). The quarterly PDSI series for the study area (1902–2005) was derived from the Dai et al. (2004) 2.5° x 2.5° monthly gridded data set (central point: 38°45'S and 71°15'W). To assess the relationships between ENSO variability and the *Araucaria* tree-ring parameters evaluated in this study, we utilized the sea surface temperatures (SSTs) from El Niño-3 region provided by ESRL/NOAA (https://psl.noaa.gov/gcos_wgsp/Timeseries/Nino3/, period: 1950–2018). We utilised the SAM index developed by Marshall (2003), https://legacy.bas.ac.uk/met/gjma/sam.html, period: 1957–2017) to evaluate the relationships between the Southern Annular Mode and the *Araucaria* tree-ring parameters. All comparisons were made for the common period 1950–2005, except for the SAM index, which begins in 1957.

Additionally, spatial correlation analyses were conducted to determine the spatial domains of the relationships between ring parameters and climate. Hence, the spatial correlation patterns between tree ring parameters and different combinations of seasonal temperature, precipitation, sea surface temperatures (SSTs) and 850 geopotential heights gridded data (0.5 × 0.5∘ grid) were investigated using the CRU TS database (Mitchell and Jones, 2005) available from Climate Explorer at the Royal Netherlands Meteorological Institute (KNMI; Trouet and van Oldenborgh, 2013). Then, the correlation maps were displayed with QGIS Desktop (v 3.4.13).

3. Results

3.1. Common signal level and association between chronologies

First, to compare the degree of common signal between samples as a measure of population synchrony, we evaluated the RBARs per parameter and methodological approach (Table 1). Among the blue parameters, EWBI exhibited the highest degree of common signal for all three methods (mean = 0.319 ± 0.014). For all BI parameters, the Mean method (average of the series obtained by LR) showed the highest degree of common signal (mean= 0.468 ± 0.042), although no significant differences in the mean RBAR were found between them (F=0.624, p = 0.619). The series displayed a higher degree of association in RW compared to the BI parameters.

Table 1
Mean RBAR of the residual chronologies in the various tree-ring parameters measured using different methodological approaches. See Materials and methods for methodological approach code definitions.

Parameter*	C_{100} (n = 20)	C_{200} (n = 20)	LR (n = 40)	Mean (n = 20)
EWBI	0.291	0.315	0.310	0.359
LWBI	0.238	0.263	0.256	0.301
DBI	0.186	0.208	0.200	0.236
RW	0.411			

* Parameters: EWBI, earlywood BI; LWBI, latewood BI; DBI, delta BI; and RW, ring width

The non-detrended EWBI and LWBI chronologies exhibit a declining trend (Fig. 3) which is also observed for RW, although in this case, greater variability in ring width was found in the early years of the chronology. In the case of the DBI chronology no age-dependent trend over time was observed. Standardisation by age-dependent spline curves, coupled with the application of autoregressive modelling (residual chronologies), eliminates all long-term trends, but retains sub-decadal and inter-annual variation very well.

To analyse the stability of the degree of common signal over time and how the expressed signal of the sample degrades with replication, the temporal evolution of RBAR and EPS was analysed for the different BI parameters compared to RW, according to the experimental methods (Fig. 4). Compared to the residual chronologies of LWBI and DBI, which had initial portions with EPS values below the 0.85 threshold, the EWBI chronology showed the greatest stability in the common signal between samples. For RW, the residual chronology is reliable from 1820 to the present. Considering the different BI parameters, the LR configuration showed the best temporal signal stability, with RBAR and EPS slightly higher in the early portions of the chronologies (the temporal evolution of RBAR exhibited very similar variations between BI methodologies).

To assess the degree of similarity between the chronologies generated by the various treatments for each tree-ring parameter, correlation matrices were constructed to facilitate visualisation and comparison (Figs. S3 and 5). For each of the BI parameters considered, the degree of similarity among the residual chronologies obtained in the four treatments was very high, with no case lower than 0.91 (Fig. S3). When the different BI parameters were compared with each other and with RW to assess their similarity, all associations were significant, except for the correlation between LWBI and RW. EWBI and LWBI were positively correlated and exhibited the highest association value (Fig. 5). This earlywood parameter was negatively correlated with DBI and RW. Conversely, DBI was positively correlated with both LWBI and RW.

3.2. Relationships between climate and tree-ring variables

Correlation functions showed similarities in the relationships between BI parameters and climate (Fig. 6). Variations in the responses between chronologies developed with different methodological treatments were practically negligible, as indicated by the small standard errors of the mean correlations. All BI parameters were significantly positively correlated with temperature and significantly negatively correlated with precipitation and PDSI. In the case of EWBI, these associations were stronger during the spring of the growing season. In contrast, the strongest association of LWBI with climatic variables occurred during the summer, with this parameter showing the highest correlation with precipitation and PDSI. For DBI, the associations with climatic variables were also strongest during the summer, and the highest correlation was observed with temperature. However, in the

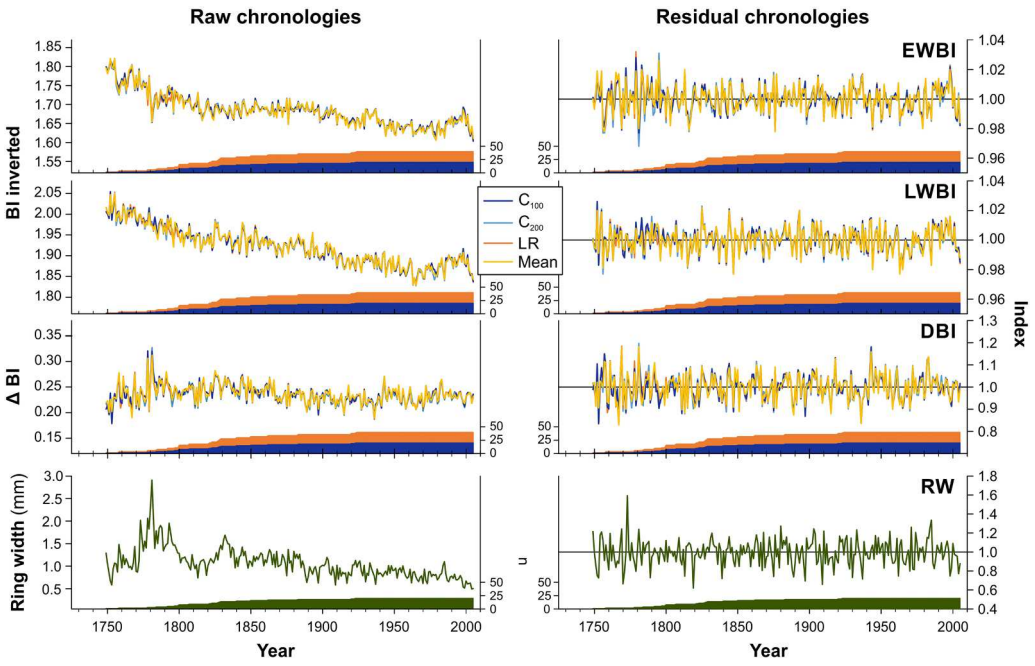

Fig. 3. RAW and residual chronologies for the tree-ring variables (EWBI, earlywood BI; LWBI, latewood BI; DBI: delta BI; RW: ring width). The central legend displays the colour corresponding to each BI methodological approach (see text for method code definitions). Sample size is represented by the shaded colour areas at the bottom of each panel.

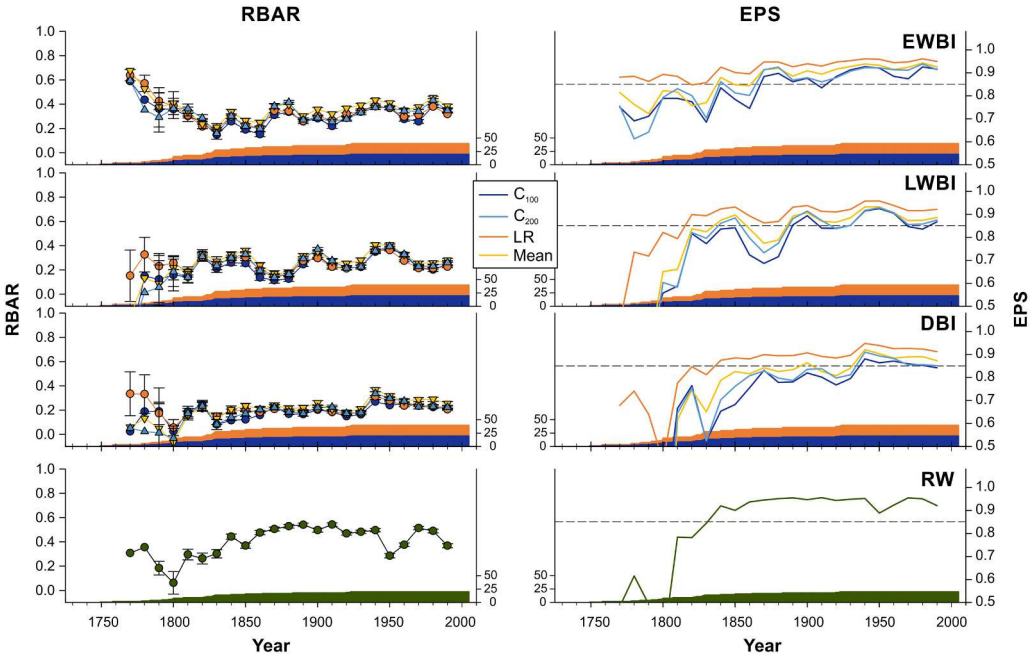

Fig. 4. Running RBAR (left panels) and EPS (right panels) statistics for the residual chronologies of earlywood BI (EWBI), latewood BI (LWBI), delta BI (DBI), and ring width (RW). The central legend displays the colour corresponding to each BI methodological approach (see text for method codes). The values were calculated for 20-year windows with a 10-year overlap. For RBAR, each point represents the mean values with their respective standard errors. Sample size is represented by the shaded colour areas at the bottom of each panel.

case of RW, there was no significant correlation with climatic parameters.

Correlation functions were also employed to assess the relationship between the large-scale atmospheric circulation modes affecting North Patagonia (ENSO and SAM) and different tree-ring parameters (Fig. 7). For the BI variables, positive relationships were found between Niño 3 SST and LWBI and between Niño 3 SST and DBI for the fall (MAM) preceding the start of the growing season. In contrast, SAM was significantly positively associated with EWBI and LWBI during the current summer, with the highest association with the former. ENSO and SAM circulation modes were inversely associated with RW. DBI showed no significant relationship with SAM.

Spatial correlation maps were used to assess the most extensive geographic dominance or area of influence between the BI variables (Fig. 8). The strongest association (higher correlation coefficients and larger spatial dominance) with temperature occurs for the mean of the

	EWBI	LWBI	DBI	RW
EWBI		**0.553**	**-0.318**	**-0.452**
LWBI	**0.549**		**0.475**	-0.013
DBI	**-0.375**	**0.470**		**0.443**
RW	**-0.449**	-0.024	**0.457**	

Fig. 5. Correlation matrix between the mean of the residual chronologies from the different blue parameters (EWBI, LWBI, and DBI) and the RW chronology. Correlation coefficients in the upper right triangle correspond to Spearman's coefficients, while those in the lower left triangle correspond to Pearson's coefficients. Bold numbers indicate significant values at the 0.05 significance level.

residual DBI chronologies during the current summer (DJF). In this case, a significant positive correlation was observed across the entire Patagonian region (Fig. 8a). Precipitation displayed a relatively more localised pattern, with its most significant association identified between the mean of the residual EWBI chronologies and rainfalls during the current spring season (SON). In this instance, the highest significant negative spatial correlations were observed near the study area, primarily within the Andes Mountain range that naturally separates Argentina and Chile (Fig. 8b). Lastly, the PDSI showed its best spatial association with the mean of the residual LWBI chronologies during the current summer (Fig. 8c). For this drought index, the association was stronger than that observed for precipitation, but considerably more geographically limited along the Patagonian Andes.

To identify the climatic spatial patterns consistent with ENSO and SAM influences on BI variations, spatial correlations were also determined between the BI chronologies and SST and the 850 mb geopotential height across the Southern Hemisphere between 160°W and 30°E (Fig. 9). Concerning the relationships with SST, the strongest correlation with the mean of the residual LWBI chronologies occurred for fall (MAM) preceding the growing season (Fig. 9a). A large oceanic region with significant positive correlations is located within the equatorial Pacific Ocean domain, spanning from 140° to 80°W. For atmospheric pressure, the strongest correlation pattern resulted from comparing the mean of the EWBI residual chronologies with the 850 mb geopotential height during summer (DJF) in the current growing season (Fig. 9b). A contrasting low- versus high-latitude spatial pattern emerged, featuring positive correlations over the Pacific Ocean between 130 and 100°W and 30°−45°S and negative correlations at high latitudes (60–80°S) over Antarctica and the surrounding Southern Ocean.

4. Discussion

In this study, we statistically evaluated the effect of the frame width (100 or 200 dpi, i.e. 20 or 40% of the core width), replication (one or two frames) and position (one central versus two frames on the left and right core sectors without overlapping) on the development of blue intensity (BI) chronologies based on different parameters (earlywood, latewood, and delta BI) in *Araucaria*. These BI chronologies were compared with the corresponding ring width (RW) chronology, and differences in the relationships with climate were assessed between the different BI chronologies. Using classical statistics to evaluate the strength of the common signal (RBAR and EPS), we found that series duplication and averaging (Mean method) produced the strongest common signal for the different blue parameters. Furthermore, doubling the window size improved the common signal. However, all BI chronologies obtained by the four methodological approaches were strongly correlated, indicating that they essentially express the same variability. In terms of effort (time) and bias due to a potential pseudo-replication effect, our results suggest that the C_{200} method (200 dpi wide window or 40% of the core width in a central position) would be the most recommended approach in *Araucaria* BI studies. In addition, the *Araucaria* BI series provided complementary information and a higher degree of

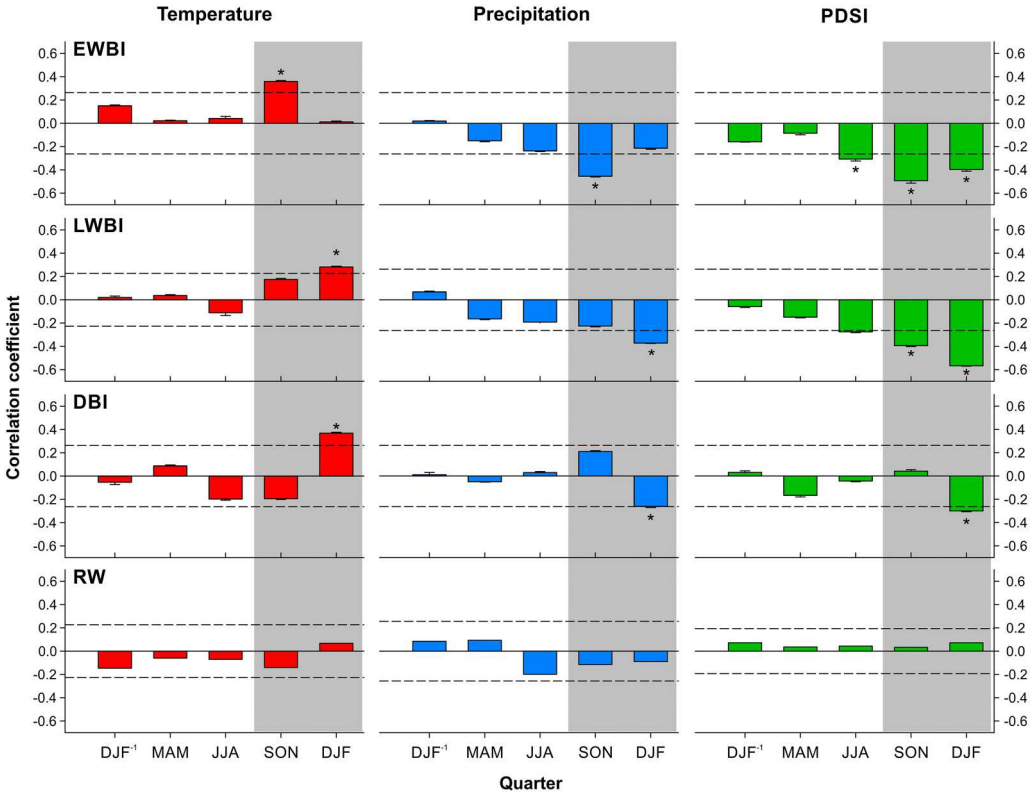

Fig. 6. Mean correlation coefficients (bars) and standard errors (capped lines) resulting from averaging the correlations between the residual chronologies (EWBI, LWBI, DBI and RW from top to bottom) from the four methodological approaches and quarterly mean temperature (left panels), total precipitation (central panels) and mean PDSI (right panels) variations as determined by correlation functions over the common period 1950–2005. The grey areas represent the current year growing season (September–February) and the dashed lines the 95% confidence limits.

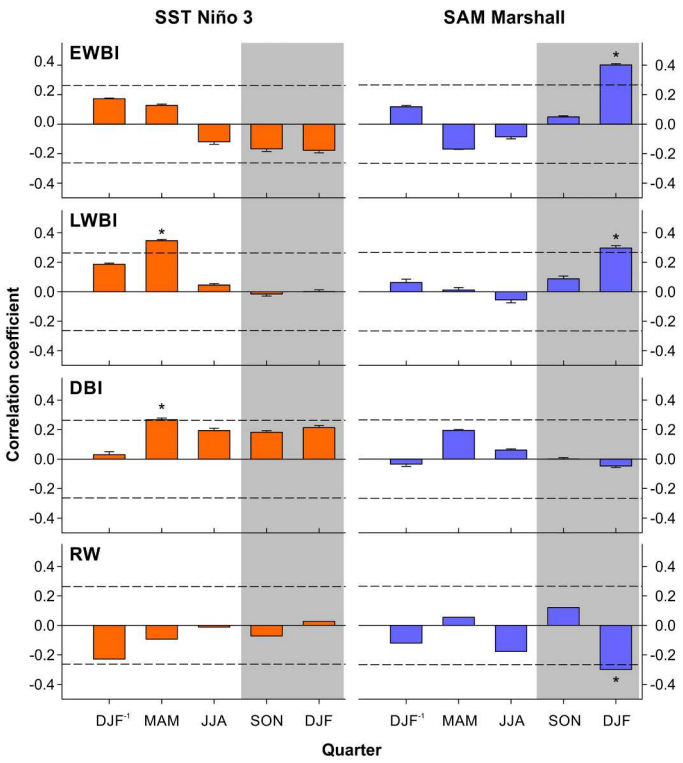

Fig. 7. Mean correlation coefficients (bars) and standard errors (capped lines) resulting from averaging the correlations between the residual tree-ring chronologies (EWBI, LWBI, DBI and RW from top to bottom) from the four methodological approaches and quarterly SST Niño 3 (1950–2005; left panels) and SAM Marshall (1957–2005; right panels) indices variations as determined by correlation functions. The grey areas represent the current year growing season (September–February) and the dashed lines the 95% confidence limits.

association with climatic variables compared to RW, highlighting the importance of this parameter in terms of climatic and ecophysiological reconstructions based on this species.

Regardless of the method used, the mean RBARs for the different BI parameters (EWBI, LWBI, and DBI) were lower than for the RW as already described for other species. This was generally attributed to the fact that the inter-annual variance (coefficient of variation) in BI data is generally extremely low compared to RW, so any noise (i.e. changes in wood colour, Björklund et al., 2019) has a big impact resulting in a lower degree of common signal between series (Wilson et al., 2021). However, the mean RBARs for the different *Araucaria* BI parameters are comparatively higher than those reported in pioneering BI studies. For example, the average intercorrelation values reported for *Manoao colensoi* in New Zealand, even with a smaller sample size and after sample selection comparable to our study, were lower for the same BI parameters (Blake et al., 2020). This shows that preselection of samples based on (1) colour homogeneity, (2) proper placement of windows within the ring despite wavy ring edges (Figs. S2), and (3) trimming of series to remove fungus-stained portions, were useful in improving the common signal in *Araucaria*. The comparison between the BI parameters showed that, regardless of the method used, the highest common signal was obtained in the measurement of earlywood, i.e. EWBI. As confirmed by Björklund et al. (2017) on a global scale and for a large number of conifer species, tracheid size is the main driver of interannual variability in earlywood density, while cell wall thickness is the more influential factor for latewood density. Consequently, in terms of interannual variability, tracheid size in earlywood tends to be less variable between trees than cell wall thickness in latewood (Rathgeber, 2017). This would partially explain why EWBI had a common signal higher than LWBI and DBI (which is derived from the combination of both). However, this could also be due to the different depth of the earlywood collection window of the EWBI compared to the LWBI (degree of penetration) or just random aspects associated with the samples used in this study. The temporal evolution of EPS shows that the experimental method has an effect on this statistical parameter, with the LR method consistently producing residual chronologies with EPSs above 0.85 for all three BI parameters over the same period as RW. This is a clear consequence of the effect of doubling the sample size (n), since in the LR method, the L and R tracks are considered independently, and all methods have similar RBARs over time. Since the Mean method produced the highest average RBARs for all the BI parameters, measuring two series per sample would be the best way to increase the EPS above a certain threshold. However, this method involves doubling the measurements (i.e. doubling the n) and considering that the final BI chronologies are significantly associated with each other (mean correlation coefficients >0.91), it can be stated that there is no significant improvement related to this approach. Therefore, for further BI studies in *Araucaria*, we recommend generating a single series based on windows of 40% of the ring width (in this case, 200 dpi), since among the experimental methods considering one series per sample, the C200 method provided the highest mean correlation among all BI parameters. However, when increasing the window size, we urge caution for samples with wavy annual rings. In those situations, it would also be advisable to reduce the window frame to 20% of the ring width (in this case, 100 dpi).

4.1. BI parameters in Araucaria in relation to climatic variability

In terms of their relationship with climatic variables, the *Araucaria* BI parameters showed significant associations for different months of the year and stronger associations to those recorded for RW (ring width). The BI parameters were mainly influenced by climatic variability during the current growing season, whereas RW is known to be influenced by climatic conditions in the previous growing season, both in Argentina (Hadad et al., 2015; Mundo et al., 2012b) and Chile (Muñoz et al., 2014). As expected, EWBI was associated with spring climate conditions (SON), while LWBI was related to summer conditions (DJF).

The strongest association with temperature was recorded for DBI during summer (DJF). This parameter, calculated as the difference between the maximum and minimum BI values for the latewood and earlywood in the same year, respectively, was introduced by Björklund et al. (2014) as a way to address problems in conifer xylem related to differences in colouration between heartwood and sapwood or due to discolouration caused by resin or fungi staining. DBI has shown significant success in developing temperature reconstructions based on conifers in different parts of the world (Björklund et al., 2014; Davi et al., 2021; Reid and Wilson, 2020; Wilson et al., 2017). In terms of spatial correlation patterns (Fig. 8a), the climatic domain associated with the DBI chronology extends over the whole Argentine and Chilean Patagonia.

The strongest negative relationships between EWBI and precipitation occurs in spring (SON). Spatially (Fig. 8b), gridded correlations showed that the area of spring precipitation associated with mean EWBI variability is more restricted compared to temperature with the higher correlations towards the western Patagonian region. This is due to the strong west-to-east precipitation gradient across the region in response to the greater influence of Pacific air masses, combined with the topographic barrier created by the Andes. (Prohaska, 1976; Viale et al., 2019). In consequence, the total annual precipitation decreases exponentially from the Andes to the eastern Patagonia plateau (Lenaerts et al., 2014; Paruelo et al., 1998; Viale et al., 2019).

In terms of species response, the relationship between EWBI and spring rainfall suggests that *Araucaria* produces less dense earlywood with higher spring rainfall. This could be due to the formation of tracheids with larger lumens, as proposed by Björklund et al. (2017). This is consistent with increased water demand and larger transport of dissolved minerals through the xylem at the beginning of the growing

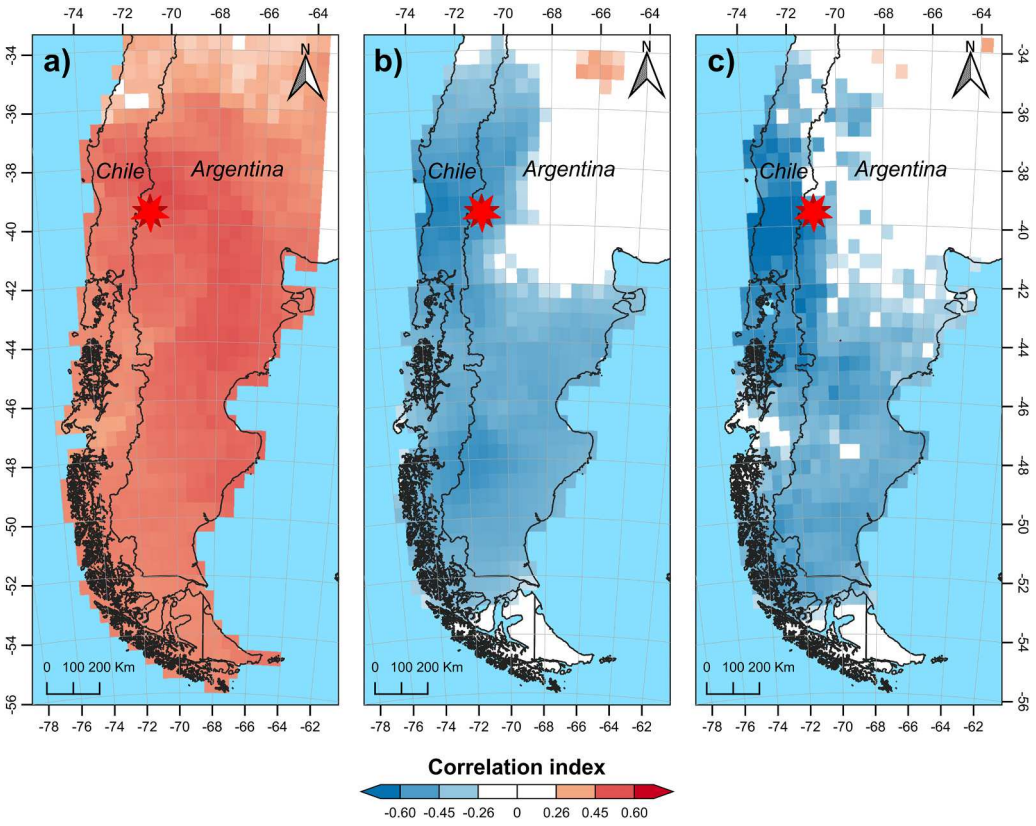

Fig. 8. Extensive spatial correlation patterns between BI chronologies and gridded climate data for a) summer CRU TS4.07 temperature (DJF), b) CRU TS4.07 spring precipitation (SON) and c) summer CRU scPDSi over the 1950–2005 common period. In (a) the most extensive correlation spatial pattern was obtained with the mean of the residual DBI chronologies, in (b) with the mean of the residual EWBI chronologies, and in (c) with the mean of residual LWBI chronologies. The maps were created with the KNMI Climate Explorer facilities and displayed with QGIS Desktop (v 3.4.13). Coloured gridded areas over the SA continent reflect significance at $p <= 0.05$. The red double star icon points the sampling site.

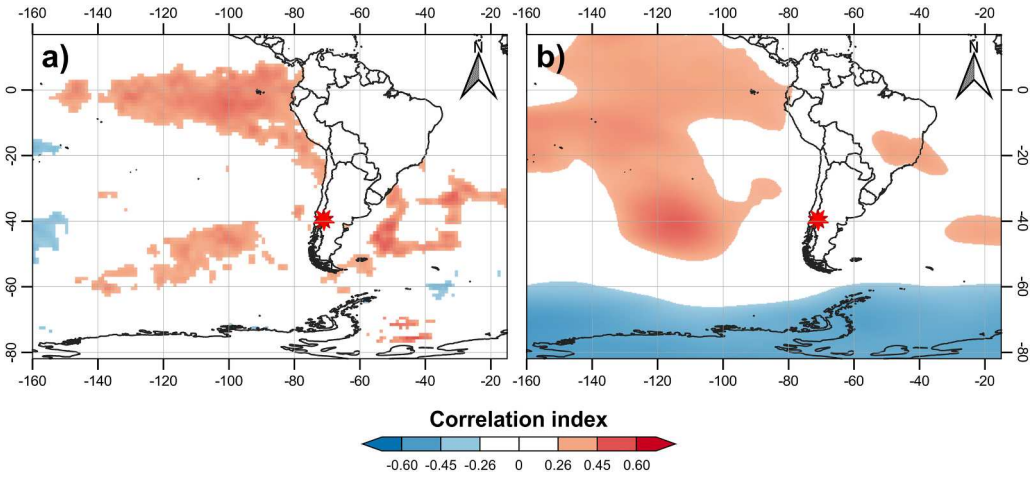

Fig. 9. Spatial correlation patterns between (a) the mean of LWBI residual chronologies with previous growing season fall (MAM) gridded SSTs (Hadley Centre Sea Ice and Sea Surface Temperature, HadlSST1), and (b) the mean of EWBI residual chronologies with current summer (DJF) gridded ERA5 850 geopotential heights for the common period 1950–2005. The maps were created with the KNMI Climate Explorer facilities and displayed with QGIS Desktop (v 3.4.13). Coloured areas reflect significance ($p <= 0.05$). Pearson correlation coefficients were computed based on the 1950–2005 common period among the dataset. The red double star icon points the sampling site.

season. Conversely, water deficit at the beginning of the growing season results in denser earlywood (Vaganov et al., 2009). Such dense earlywood is characterised by tracheids with narrow lumens and reduced hydraulic conductivity (Domec et al., 2009). Similarly, Camarero et al., (2017, 2014) found that minimum wood density showed a strong negative response to spring precipitation in conifer species from arid Mediterranean and Eurasian regions.

Overall, maximum latewood density as a proxy for precipitation has rarely been investigated (Rocha et al., 2020). In our study, summer precipitation (DJF) was also negatively associated with latewood density. Contrasting relationships between temperature (positive) and precipitation (negative) with maximum latewood density (as measured by

LWBI) could be related to summer water deficit resulting from abundant precipitation and warmer temperatures. However, the opposite relationships between summer temperature and precipitation across the Andes may exacerbated this contrasting pattern. Similar relationships have also been described in China for *Larix sibirica* in the Altay Mountains (Chen et al., 2012) and for *Larix speciosa* in the northwestern Yunnan Province (Deng et al., 2022).

Consistent with the previously described relationships between BI chronologies and precipitation, negative relationships with PDSI were also recorded during the growing season. Consequently, a positive soil water balance during the growing season negatively affects wood density, i.e. larger earlywood tracheid lumens (Begović et al., 2020) and thinner latewood cell walls. The relationships between drought indices and BI have not been widely studied (Akhmetzyanov et al., 2023). Our results are consistent to those observed by Zheng et al. (2023) in four species of *Picea* and *Abies* in central and western China, respectively. In that study, scPDSI showed a universal positive influence on EWBR (i.e. earlywood blue light reflectance following the convention proposed by Björklund et al., *in submission*) at four sites and a negative relationship with LWBI at the end of the growing season. Begovic et al. (2020) also found a positive relationship between EWBR of *Picea abies* and *Abies alba* and PDSI during the growing season. If EWBI is considered as a proxy inversely proportional to the size of earlywood cell lumens, our results are consistent with the reduction of conifer xylem lumens found in response to increasing temperature and drought in arid environments (Eilmann et al., 2009; Fonti and Babushkina, 2016; Olano et al., 2014). The associations between LWBI and summer scPDSI were much more spatially restricted than precipitation, with their maximum values close to the study site (Fig. 8c). This is in line with spatial variations and the precipitation gradient in Patagonia, as described above.

In terms of *Araucaria* BI associations with large-scale atmospheric circulation modes, the marginal positive associations between the SST Niño 3 during the previous fall (MAM) and LWBI do not align with previously described water deficit situations associated with higher densities of both early and latewood. Possibly, these marginal associations may reflect the location of our study area at the southern boundary of the ENSO influence in South America, making its effect weak and still complex to interpret. Nevertheless, the spatial correlation map for previous autumn (Fig. 9a) showed a pattern of association with SST in the equatorial Pacific off the coast of Peru, resembling the typical of El Niño events.

The EWBI and LWBI chronologies showed a significant negative relationship with the current summer SAM (Southern Annular Mode) index. This pattern was also noted in the corresponding RW chronology, as previously elucidated by Mundo et al. (2012b) in their *Araucaria* regional scale analysis. The correlation between SAM and precipitation is negative, as higher SAM index values correspond to drier conditions in northern Patagonia (Garreaud et al., 2009). The correlations with SAM are significant and consistent with those found for precipitation and PDSI. The association between *Araucaria* BI and SAM is in line with the gridded correlation map between the LWBI chronology and geopotential height at 850 mb during the summer season. The correlation map exhibits contrasting pressure areas across the mid-latitude south Pacific Ocean and the high-latitude sub-Antarctic region, indicative of SAM (Fig. 9b).

4.2. Future studies

The results of this study show great potential for the use of *Araucaria* BI variables for the development of climate sensitive chronologies applicable in ecological and climatic studies. Firstly, it is recommended to replicate this study to encompass the various environmental conditions where the species occurs. This can be achieved by establishing a network of sites that measure BI, potentially analysing the same samples from the RW network developed by Mundo et al. (2012b). Such an approach would enable a comprehensive comparison of the BI signal throughout the entire distribution of *Araucaria* in Argentina. Additionally, further investigation is required to identify the wood anatomical characteristics that are most strongly correlated with BI variation within the tree ring. This can be achieved through additional methods such as quantifying anatomical parameters.

5. Conclusions

Our work represents the first attempt to developed robust BI chronologies in southern South America. The study demonstrates the possibility of developing reliable BI chronologies from *Araucaria* forests in the Patagonian Andes. Although different methodological approaches analysing the sensitivity to changes in the window frame for BI calculation were tested, they provide quite similar results. Even though the LR method led to an improvement in the EPS statistics, this must be assessed with caution since doubling the sample size increase the EPS values and do not represent a real improvement in common signal. Therefore, we suggest to calculate the BI in the core central positions with windows covering approximately 40% of the total core width (in this case 200 dpi). Our results showed the presence of a consistent climate signal in both earlywood (EWBI) and latewood (LWBI) BI records, corresponding to the current spring and summer climate, respectively. In addition, soil water availability was significantly associated with wood density variation. The BI measurements in *Araucaria* provide climatic and environmental information that complements the data obtained from RW and density variation in early and latewood, thus obtaining intra-annual data. This creates a new avenue of research, which allows for advances in the eco-physiological understanding of the species and the development of chronologies that lead to more reliable environmental and hydroclimatic reconstructions.

CRediT authorship contribution statement

I.A. Mundo: Writing – review & editing, Writing – original draft, Resources, Project administration, Methodology, Investigation, Funding acquisition, Conceptualization. **R. Villalba**: Writing – review & editing, Project administration, Investigation, Funding acquisition. **S. Velez**: Writing – review & editing, Methodology, Formal analysis. **R. Wilson**: Writing – review & editing, Supervision, Methodology, Funding acquisition, Conceptualization.

Declaration of Competing Interest

The authors declare that they have no known competing financial interests or personal relationships that could have appeared to influence the work reported in this paper.

Data availability

Data will be made available on request.

Acknowledgements

This research was funded by the Consejo Nacional de Investigaciones Científicas y Técnicas of Argentina (Barberena PIP 0784-CONICET), the Agencia Nacional Promoción de Ciencia y Tecnología of Argentina (PICT 2018–03691), Red BOSQUE-CLIMA (Proyectos Federales de Alto Impacto of the Argentinean Ministry of Science, Technology and Innovation, contribution number 4), the BNP Paribas Foundation (THEMES project) and the National Science Foundation (grant no. 1832483). I.A. M. was also supported by the Deutsche Forschungsgemeinschaft (DFG, German Research Foundation) under Germanýs Excellence Strategy—EXC 2150–390870439. I.A.M. joined the EXC 2150 at Kiel University, Germany (June-July 2023) as a guest scientist and wrote the final version of this article during that time. We thank the Dirección Provincial de Bosques of Neuquén province and the owner of Nahuel

Mapi site for sampling permissions. We also thank the Guest editor, Jesper Björklund, and two anonymous reviewers for help to improve this manuscript.

Appendix A. Supporting information

Supplementary data associated with this article can be found in the online version at doi:10.1016/j.dendro.2024.126177.

References

Aguilera-Betti, I., Muñoz, A.A., Stahle, D., Figueroa, G., Duarte, F., González-Reyes, Á., Christie, D., Lara, A., González, M.E., Sheppard, P.R., Sauchyn, D., Moreira-Muñoz, A., Toledo-Guerrero, I., Olea, M., Apaz, P., Fernandez, A., 2017. The first millennium-age *Araucaria araucana* in Patagonia. Tree-Ring Res. 73, 53–56. https://doi.org/10.3959/1536-1098-73.1.53.

Akhmetzyanov, L., Sánchez-Salguero, R., García-González, I., Domínguez-Delmás, M., Sass-Klaassen, U., 2023. Blue is the fashion in Mediterranean pines: new drought signals from tree-ring density in southern Europe. Sci. Total Environ. 856, 159291 https://doi.org/10.1016/j.scitotenv.2022.159291.

Begović, K., Rydval, M., Mikac, S., Čupić, S., Svobodova, K., Mikoláš, M., Kozák, D., Kameniar, O., Frankovič, M., Pavlin, J., Langbehn, T., Svoboda, M., 2020. Climate-growth relationships of Norway Spruce and silver fir in primary forests of the Croatian Dinaric mountains. Agric. For. Meteorol. 288–289, 108000 https://doi.org/10.1016/j.agrformet.2020.108000.

Björklund, J., Seftigen, K., Schweingruber, F., Fonti, P., von Arx, G., Bryukhanova, M.V., Cuny, H.E., Carrer, M., Castagneri, D., Frank, D.C., 2017. Cell size and wall dimensions drive distinct variability of earlywood and latewood density in Northern Hemisphere conifers. N. Phytol. 216, 728–740. https://doi.org/10.1111/nph.14639.

Björklund, J., von Arx, G., Nievergelt, D., Wilson, R., Van den Bulcke, J., Günther, B., Loader, N.J., Rydval, M., Fonti, P., Scharnweber, T., Andreu-Hayles, L., Büntgen, U., D'Arrigo, R., Davi, N., De Mil, T., Esper, J., Gärtner, H., Geary, J., Gunnarson, B.E., Hartl, C., Hevia, A., Song, H., Janecka, K., Kaczka, R.J., Kirdyanov, A.V., Kochbeck, M., Liu, Y., Meko, M., Mundo, I., Nicolussi, K., Oelkers, R., Pichler, T., Sánchez-Salguero, R., Schneider, L., Schweingruber, F., Timonen, M., Trouet, V., Van Acker, J., Verstege, A., Villalba, R., Wilmking, M., Frank, D., 2019. Scientific merits and analytical challenges of tree-ring densitometry. Rev. Geophys. 57, 1224–1264. https://doi.org/10.1029/2019RG000642.

Björklund, J.A., Gunnarson, B.E., Seftigen, K., Esper, J., Linderholm, H.W., 2014. Blue intensity and density from northern Fennoscandian tree rings, exploring the potential to improve summer temperature reconstructions with earlywood information. Clim 10, 877–885. https://doi.org/10.5194/cp-10-877-2014.

Blake, S.A.P., Palmer, J.G., Björklund, J., Harper, J.B., Turney, C.S.M., 2020. Palaeoclimate potential of New Zealand *Manoao colensoi* (silver pine) tree rings using blue-intensity (BI). Dendrochronologia 60, 125664. https://doi.org/10.1016/j.dendro.2020.125664.

Blasing, T.J., Solomon, A.M., Duvick, D.N., 1984. Response function revisited. Tree Ring Bull. 44, 1–15.

Camarero, J.J., Rozas, V., Olano, J.M., 2014. Minimum wood density of *Juniperus thurifera* is a robust proxy of spring water availability in a continental Mediterranean climate. J. Biogeogr. 41, 1105–1114. https://doi.org/10.1111/jbi.12271.

Camarero, J.J., Fernández-Pérez, L., Kirdyanov, A.V., Shestakova, T.A., Knorre, A.A., Kukarskih, V.V., Voltas, J., 2017. Minimum wood density of conifers portrays changes in early season precipitation at dry and cold Eurasian regions. Trees 31, 1423–1437. https://doi.org/10.1007/s00468-017-1559-x.

Chen, F., Yuan, Y., Wei, W., Fan, Z., Zhang, T., Shang, H., Zhang, R., Yu, S., Ji, C., Qin, L., 2012. Climatic response of ring width and maximum latewood density of *Larix sibirica* in the Altay Mountains, reveals recent warming trends. Ann. For. Sci. 69, 723–733. https://doi.org/10.1007/s13595-012-0187-2.

Cook, E.R., Holmes, R.L., 1986. User's manual for program ARSTAN. Tree-ring chronologies of western North America: California, eastern Oregon and northern Great Basin, pp. 50–65.

Dai, A., Trenberth, K.E., Qian, T., 2004. A global dataset of Palmer drought severity Index for 1870–2002: relationship with soil moisture and Effects of Surface Warming. J. Hydrometeorol. 5, 1117–1130.

Davi, N.K., Rao, M.P., Wilson, R., Andreu-Hayles, L., Oelkers, R., D'Arrigo, R., Nachin, B., Buckley, B., Pederson, N., Leland, C., Suran, B., 2021. Accelerated recent warming and temperature variability over the past eight centuries in the central asian Altai from blue intensity in tree rings. Geophys. Res. Lett. 48, e2021GL092933 https://doi.org/10.1029/2021GL092933.

Deng, G., Li, M., Hao, Z., Shao, X., 2022. Responses to climate change of maximum latewood density from *Larix speciosa* Cheng et Law and *Abies delavayi* Franch. in the northwest of Yunnan province, China. Forests 13. https://doi.org/10.3390/f13050720.

Diaz-Vaz, J.E., Devlieger, F., Poblete, H., Juacida, R., 2002. Maderas comerciales de Chile, Tercera edición. ed. Marisa Cúneo Ediciones, Valdivia, Chile.

Domec, J.-C., Warren, J.M., Meinzer, F.C., Lachenbruch, B., 2009. Safety factors for xylem failure by implosion and air-seeding within roots, trunks and branches of young and old conifer tees. IAWA J. 30, 101–120. https://doi.org/10.1163/22941932-90000207.

Eilmann, B., Zweifel, R., Buchmann, N., Fonti, P., Rigling, A., 2009. Drought-induced adaptation of the xylem in Scots pine and pubescent oak. Tree Physiol. 29, 1011–1020. https://doi.org/10.1093/treephys/tpp035.

Fonti, P., Babushkina, E.A., 2016. Tracheid anatomical responses to climate in a forest-steppe in Southern Siberia. Dendrochronologia 39, 32–41. https://doi.org/10.1016/j.dendro.2015.09.002.

Fritts, H.C., 1976. Tree Rings and Climate. Academic Press, London.

Garreaud, R.D., Vuille, M., Compagnucci, R., Marengo, J., 2009. Present-day South American climate. Palaeogeogr. Palaeocl. 281, 180–195. https://doi.org/10.1016/j.palaeo.2007.10.032.

González, M.E., Veblen, T.T., Sibold, J.S., 2005. Fire history of *Araucaria-Nothofagus* forests in Villarrica National Park, Chile. J. Biogeogr. 32, 1187–1202.

Hadad, M.A., Roig Juñent, F.A., Boninsegna, J.A., Patón-Domínguez, D., 2015. Age effects on the climatic signal in *Araucaria araucana* from xeric sites in Patagonia, Argentina. Plant Ecol. Divers. 8, 343–351.

Hadad, M.A., Arco Molina, J.G., Roig, F.A., 2020. Dendrochronological study of the xeric and mesic *Araucaria araucana* forests of northern Patagonia: implications for ecology and conservation. In: Pompa-García, M., Camarero, J.J. (Eds.), Latin American Dendroecology: Combining Tree-Ring Sciences and Ecology in a Megadiverse Territory. Springer International Publishing, Cham, pp. 283–315. https://doi.org/10.1007/978-3-030-36930-9_13.

Hadad, M.A., Roig, F.A., Arco Molina, J.G., Hacket-Pain, A., 2021. Growth of male and female *Araucaria araucana* trees respond differently to regional mast events, creating sex-specific patterns in their tree-ring chronologies. Ecol. Indic. 122, 107245 https://doi.org/10.1016/j.ecolind.2020.107245.

Heeter, K.J., King, D.J., Harley, G.L., Kaczka, R.J., 2022. Video tutorial: measuring blue intensity with the CooRecorder software application. Dendrochronologia 76, 125999. https://doi.org/10.1016/j.dendro.2022.125999.

Holmes, R.L., 1983. Computer-assisted quality control in tree-ring dating and measurement. Tree Ring Bull. 43, 69–78.

Holmes, R.L., Stockton, C.W., LaMarche, V.C., 1979. Extension of river flow records in Argentina from long tree-ring chronologies. J. Am. Water Resour. 15, 1081–1085.

Kaczka, R.J., Wilson, R., 2021. I-BIND: International Blue intensity network development working group. Dendrochronologia 68, 125859. https://doi.org/10.1016/j.dendro.2021.125859.

Kaczka, R.J., Spyt, B., Janecka, K., Beil, I., Büntgen, U., Scharnweber, T., Nievergelt, D., Wilmking, M., 2018. Different maximum latewood density and blue intensity measurements techniques reveal similar results. Dendrochronologia 49, 94–101. https://doi.org/10.1016/j.dendro.2018.03.005.

LaMarche, V.C., Holmes, R.L., Donwiddie, P., Drew, L., 1979. Tree-ring chronologies of the southern hemisphere: 1. Argentina, Chronologies Series V. University of Arizona, Tucson.

Lara, A., Villalba, R., 1993. A 3620-year temperature record from Fitzroya cupressoides tree rings in Southern South America. Science 260, 1104–1106.

Larsson, L.-Å., 2020. CooRecorder and CDendro programs of the package CooRecorder/CDendro version 9.6.

Lavergne, A., Daux, V., Pierre, M., Stievenard, M., Srur, A.M., Villalba, R., 2018. Past summer temperatures inferred from dendrochronological records of *Fitzroya cupressoides* on the eastern slope of the northern patagonian Andes. J. Geophys. Res.: Biogeosciences 123, 32–45. https://doi.org/10.1002/2017JG003989.

Lenaerts, J.T.M., van den Broeke, M.R., van Wessem, J.M., van de Berg, W.J., van Meijgaard, E., van Ulft, L.H., Schaefer, M., 2014. Extreme precipitation and climate gradients in Patagonia revealed by high-resolution regional atmospheric climate modeling. J. Clim. 27, 4607–4621. https://doi.org/10.1175/JCLI-D-13-00579.1.

Marshall, G.J., 2003. Trends in the Southern annular mode from observations and reanalyses. J. Clim. 16, 4134–4143. https://doi.org/10.1175/1520-0442(2003)016<4134:TITSAM>2.0.CO;2.

McCarroll, D., Pettigrew, E., Luckman, A., Guibal, F., Edouard, J.-L., 2002. Blue reflectance provides a surrogate for latewood density of high-latitude pine tree rings. Arct. Antarct. Alp. Res. 34, 450–453. https://doi.org/10.1080/15230430.2002.12003516.

Melvin, T.M., Briffa, K.R., Nicolussi, K., Grabner, M., 2007. Time-varying-response smoothing. Dendrochronologia 25, 65–69. https://doi.org/10.1016/j.dendro.2007.01.004.

Mitchell, T.D., Jones, P.D., 2005. An improved method of constructing a database of monthly climate observations and associated high-resolution grids. Int. J. Climatol. 25, 693–712. https://doi.org/10.1002/joc.1181.

Morales, M.S., Cook, E.R., Barichivich, J., Christie, D.A., Villalba, R., LeQuesne, C., Srur, A.M., Ferrero, M.E., González-Reyes, Á., Couvreux, F., Matskovsky, V., Aravena, J.C., Lara, A., Mundo, I.A., Rojas, F., Prieto, M.R., Smerdon, J.E., Bianchi, L.O., Masiokas, M.H., Urrutia-Jalabert, R., Rodriguez-Catón, M., Muñoz, A. A., Rojas-Badilla, M., Alvarez, C., Lopez, L., Luckman, B.H., Lister, D., Harris, I., Jones, P.D., Williams, A.P., Velazquez, G., Aliste, D., Aguilera-Betti, I., Marcotti, E., Flores, F., Muñoz, T., Cuq, E., Boninsegna, J.A., 2020. Six hundred years of South American tree rings reveal an increase in severe hydroclimatic events since mid-20th century. Proc. Natl. Acad. Sci. USA 202002411. https://doi.org/10.1073/pnas.2002411117.

Mundo, I.A., 2011. Historia de incendios en bosques de *Araucaria araucana* (Molina) K. Koch de Argentina a través de un análisis dendroecológico (Tesis Doctoral). Universidad Nacional de La Plata, La Plata, Argentina.

Mundo, I.A., Masiokas, M.H., Villalba, R., Morales, M.S., Neukom, R., Le Quesne, C., Urrutia, R.B., Lara, A., 2012a. Multi-century tree-ring based reconstruction of the Neuquén River streamflow, northern Patagonia, Argentina. Clim 8, 815–829. https://doi.org/10.5194/cp-8-815-2012.

Mundo, I.A., Roig Juñent, F.A., Villalba, R., Kitzberger, T., Barrera, M.D., 2012b. *Araucaria araucana* tree-ring chronologies in Argentina: spatial growth variations and climate influences. Trees Struct. Funct. 26, 443–458. https://doi.org/10.1007/s00468-011-0605-3.

Mundo, I.A., Kitzberger, T., Roig Juñent, F.A., Villalba, R., Barrera, M.D., 2013. Fire history in the *Araucaria araucana* forests of Argentina: human and climate influences. Int. J. Wildland Fire 22, 194–206. https://doi.org/10.1071/WF11164.

Mundo, I.A., Wilson, R., Villalba, R., 2016. Blue intensity measurements in *Araucaria araucana* from northern Patagonia: preliminary results, in: Meeting Program and Abstracts - AmeriDendro 2016. Presented at the Third American Dendrochronology Conference - AmeriDendro 2016, Mendoza, Argentina, pp. 77–78.

Mundo, I.A., Sanguinetti, J., Kitzberger, T., 2021. Multi-centennial phase-locking between reproduction of a South American conifer and large-scale drivers of climate. Nat. Plants 7, 1560–1570. https://doi.org/10.1038/s41477-021-01038-1.

Muñoz, A.A., Barichivich, J., Christie, D.A., Dorigo, W., Sauchyn, D., González-Reyes, A., Villalba, R., Lara, A., Riquelme, N., González, M.E., 2014. Patterns and drivers of *Araucaria araucana* forest growth along a biophysical gradient in the northern Patagonian Andes: linking tree rings with satellite observations of soil moisture. Austral Ecol. 39, 158–169. https://doi.org/10.1111/aec.12054.

Neukom, R., Gergis, J., Karoly, D.J., Wanner, H., Curran, M., Elbert, J., Gonzalez-Rouco, F., Linsley, B.K., Moy, A.D., Mundo, I., Raible, C.C., Steig, E.J., van Ommen, T., Vance, T., Villalba, R., Zinke, J., Frank, D., 2014. Inter-hemispheric temperature variability over the past millennium. Nat. Clim. Change Adv. Online Publ.

Olano, J.M., Linares, J.C., García-Cervigón, A.I., Arzac, A., Delgado, A., Rozas, V., 2014. Drought-induced increase in water-use efficiency reduces secondary tree growth and tracheid wall thickness in a Mediterranean conifer. Oecologia 176, 273–283. https://doi.org/10.1007/s00442-014-2989-4.

Ols, C., Klesse, S., Girardin, M.P., Evans, M.E.K., DeRose, R.J., Trouet, V., 2023. Detrending climate data prior to climate–growth analyses in dendroecology: a common best practice? Dendrochronologia 79, 126094. https://doi.org/10.1016/j.dendro.2023.126094.

Palmer, J.G., 1965. Meteorological drought, Research Paper 45. U.S. Department of Commerce, Washington, D.C.

Paruelo, J.M., Jobbagy, E., Sala, O.E., Golluscio, R.A., 1998. The climate of Patagonia: general patterns and controls on biotic processes. Ecol. Austral 8, 85–101.

Prohaska, F., 1976. The climate of Argentina, Paraguay, and Uruguay. In: Admiraal, W. (Ed.), Climates of Central and South America - World Survey of Climatology. Elsevier, Amsterdam, Netherlands, pp. 13–112.

Rathgeber, C.B.K., 2017. Conifer tree-ring density inter-annual variability – anatomical, physiological and environmental determinants. N. Phytol. 216, 621–625. https://doi.org/10.1111/nph.14763.

Reid, E., Wilson, R., 2020. Delta blue intensity vs. maximum density: a case study using *Pinus uncinata* in the Pyrenees. Dendrochronologia 61, 125706. https://doi.org/10.1016/j.dendro.2020.125706.

Rocha, E., Gunnarson, B.E., Holzkämper, S., 2020. Reconstructing summer precipitation with MXD data from *Pinus sylvestris* growing in the Stockholm archipelago. Atmosphere 11. https://doi.org/10.3390/atmos11080790.

Rozas, V., Le Quesne, C., Rojas-Badilla, M., González-Reyes, Á., Donoso, S., Olano, J.M., 2019. Climatic cues for secondary growth and cone production are sex-dependent in the long-lived dioecious conifer *Araucaria araucana*. Agric. For. Meteorol. 274, 132–143. https://doi.org/10.1016/j.agrformet.2019.05.003.

Rydval, M., Larsson, L.A., McGlynn, L., Gunnarson, B.E., Loader, N.J., Young, G.H.F., Wilson, R., 2014. Blue intensity for dendroclimatology: Should we have the blues? experiments from Scotland. Dendrochronologia 32, 191–204. https://doi.org/10.1016/j.dendro.2014.04.003.

Schulman, E., 1956. Dendroclimatic Changes in Semiarid America. University of Arizona Press, Tucson.

Schweingruber, F.H., 1988. Tree Rings: Basics and Applications of Dendrochronology. D. Reidel Publishing Company, Derdrecht, Holland.

Tortorelli, L.A., 1956. Maderas y Bosques Argentinos. Editorial Acme, Buenos Aires.

Trouet, V., van Oldenborgh, G., 2013. KNMI climate explorer: a web-based research tool for high-resolution paleoclimatology. Tree-Ring Res. 69, 3–13. https://doi.org/10.3959/1536-1098-69.1.3.

Vaganov, E.A., Schulze, E.-D., Skomarkova, M.V., Knohl, A., Brand, W.A., Roscher, C., 2009. Intra-annual variability of anatomical structure and δ13C values within tree rings of spruce and pine in alpine, temperate and boreal Europe. Oecologia 161, 729–745. https://doi.org/10.1007/s00442-009-1421-y.

Veblen, T.T., Burns, B.R., Kitzberger, T., Lara, A., Villalba, R., 1995. The ecology of the conifers of southern South America. In: Ecology of the Southern Conifers. Melbourne. University Press, Parkville, pp. 120–155.

Viale, M., Bianchi, E., Cara, L., Ruiz, L.E., Villalba, R., Pitte, P., Masiokas, M., Rivera, J., Zalazar, L., 2019. Contrasting climates at both sides of the Andes in Argentina and Chile. Front. Environ. Sci. 7.

Villalba, R., 1990. Climatic fluctuations in Northern Patagonia during the Last 1000 Years as inferred from tree-ring records. Quat. Res. 34, 346–360.

Villalba, R., Veblen, T.T., 1997. Spatial and temporal variation in *Austrocedrus* growth along the forest-steppe ecotone in northern Patagonia. Can. J. Res. 27, 580–597.

Villalba, R., Boninsegna, J.A., Cobos, D.R., 1989. A tree-ring reconstruction of summer temperature between A.D. 1500 and 1974 in western Argentina. Presented at the Third International Conference on Southern Hemisphere Meteorology & Oceanography. Buenos Aires, pp. 196–197.

Villalba, R., Cook, E.R., Jacoby, G.C., D'Arrigo, R., Veblen, T.T., Jones, P.D., 1998. Tree-ring based reconstruction of northern Patagonia precipitation since AD 1600. Holocene 8, 659–674.

Villalba, R., Lara, A., Masiokas, M.H., Urrutia, R., Luckman, B.H., Marshall, G.J., Mundo, I.A., Christie, D.A., Cook, E.R., Neukom, R., Allen, K., Fenwick, P., Boninsegna, J.A., Srur, A.M., Morales, M.S., Araneo, D., Palmer, J.G., Cuq, E., Aravena, J.C., Holz, A., LeQuesne, C., 2012. Unusual Southern Hemisphere tree growth patterns induced by changes in the Southern Annular Mode. Nat. Geosci. 5, 793–798. https://doi.org/10.1038/ngeo1613.

Wigley, T.M.L., Briffa, K., Jones, P.D., 1984. On the average value of correlated time series, with applications in dendroclimatology and hydrometeorology. J. Clim. Appl. Meteorol. 23, 201–213.

Wilson, R., Rao, R., Rydval, M., Wood, C., Larsson, L.-Å., Luckman, B.H., 2014. Blue Intensity for dendroclimatology: The BC blues: a case study from British Columbia, Canada. Holocene 24, 1428–1438. https://doi.org/10.1177/0959683614544051.

Wilson, R., D'Arrigo, R., Andreu-Hayles, L., Oelkers, R., Wiles, G., Anchukaitis, K., Davi, N., 2017. Experiments based on blue intensity for reconstructing North Pacific temperatures along the Gulf of Alaska. Clim 13, 1007–1022. https://doi.org/10.5194/cp-13-1007-2017.

Wilson, R., Allen, K., Baker, P., Boswijk, G., Buckley, B., Cook, E., D'Arrigo, R., Druckenbrod, D., Fowler, A., Grandjean, M., Krusic, P., Palmer, J., 2021. Evaluating the dendroclimatological potential of blue intensity on multiple conifer species from Tasmania and New Zealand. Biogeosciences 18, 6393–6421. https://doi.org/10.5194/bg-18-6393-2021.

Zheng, Y., Shen, H., Abernethy, R., Wilson, R., 2023. Experiments of the efficacy of tree ring blue intensity as a climate proxy in central and western China. Biogeosciences 20, 3481–3490. https://doi.org/10.5194/bg-20-3481-2023.